EUROPEAN ORGANIZATION FOR NUCLEAR RESEARCH
European Laboratory for Particle Physics

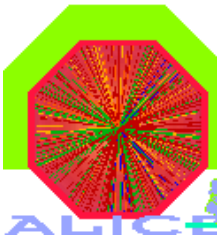

Internal Note/
ALICE reference number
ALICE-INT-2006-0002 version 1.0

2006-03-20

ALICE MUON TRIGGER PERFORMANCE

Authors:

F. Guerin[(1)], F. Yermia[(2)], P. Dupieux[(1)], P. Rosnet[(1)] and E. Vercellin[(2)]

[(1)] Laboratoire de Physique Corpusculaire, IN2P3/CNRS et Université Blaise Pascal de Clermont-Fd
[(2)] INFN sezione di Torino, Università di Torino, Dipartimento di Fisica Sperimentale

Abstract:

This document summarizes the simulated performance of the ALICE muon trigger. The simulations are performed within the AliRoot framework. The efficiency on muons from quarkonia, pions, kaons, charm and beauty hadron decays are presented. In addition, an evaluation of the trigger rates for Pb-Pb, Ar-Ar and p-p is done in view of the elaboration of physics data taking scenarii with the muon spectrometer.

1 MOTIVATIONS

The ALICE muon trigger performance was already evaluated in 1999 [1][2] when the system was still under an optimization phase. Detector segmentations and algorithms are now completely defined. The software has been significantly improved too. A detailed simulation of the setup effects can be now performed within AliRoot, which contains a full geometrical description of the muon trigger subsystem. Using these tools, the trigger transverse momentum p_T cut has been optimized in a previous work [3]. Finally, most recent parameterizations of signal and background, which are described in section 3, are available.

These arguments motivated this update of the study of the muon trigger performance. The trigger rates are calculated for Pb-Pb, Ar-Ar and p-p [4] at $\sqrt{s_{NN}}$ = 5.5 TeV, 6.3 TeV and 14 TeV, respectively. For each system, the considered luminosity and collision frequency are indicated in Table 1 (from [5]). Of course, the trigger rates scale directly with luminosity.

	Pb-Pb $\sqrt{s_{NN}}$ = 5.5 TeV	Ar-Ar $\sqrt{s_{NN}}$ = 6.3 TeV	p-p $\sqrt{s_{NN}}$ = 14 TeV
<L> (cm^{-2} s^{-1})	$5\ 10^{26}$	$5\ 10^{28}$	$3\ 10^{30}$
f^{coll} (Hz)	$4\ 10^{3}$	$1.5\ 10^{5}$	$2\ 10^{5}$

Table 1 : Mean luminosity <L> and corresponding number of inelastic collisions per second f^{coll} considered for the evaluation of the trigger rates for Pb-Pb, Ar-Ar and p-p collisions.

The trigger rates are calculated for given assumptions on background yields. It will be demonstrated that, as expected, the trigger probability obeys simple Poisson statistics so that scaling to different background conditions is rather straightforward.

This note refers to the L0 muon trigger only: the muon High Level Trigger (HLT), which should reduce the permanent storage rate by filtering the events selected by the L0 trigger, is not considered here.

2 TRIGGER ALGORITHM

The muon trigger is based on single gap RPCs (Resistive Plate Chambers), which are position sensitive detectors (few mm resolution) with very good time resolution (less than 2 ns). The muon trigger electronics and algorithm are described in detail in [6]. A brief summary is given in this section.

The trigger algorithm is performed by means of a dedicated electronics. Basically, tracks pointing approximately back to the primary interaction vertex are searched for, using the information of four RPC detector planes. At least 3 fired detector planes out of 4 are required to define a track, both in the bending and non-bending plane. The non-bending plane algorithm is very effective for background rejection. In the bending plane, the track deviation relative to a particle with infinite momentum is computed. Subsequent cuts on this deviation, performed by means of LUT (Look-up-Tables), allow rejecting low p_T particles which have obviously large

deviations. These two cuts, named low p_T (l-pt) and high p_T (h-pt) cuts, are loaded in the LUT. Finally, the six following trigger signals are delivered to the ALICE Central Trigger Processor, less than 800 ns after interaction, at 40 MHz frequency:

- At least one single muon [1] above low (high) p_T cut, called "single muon low (high) p_T";
- At least two muons with opposite deviation signs, each of them above low (high) p_T cut, called "unlike-sign dimuon low (high) p_T";
- At least two muons with same deviation signs, each of them above low (high) p_T cut, called "like-sign dimuon low (high) p_T".

In the particular case where the computed deviation is zero, associated tracks are considered belonging to both classes of sign by the algorithm.

The results presented in this document correspond to particular cases of the l-pt and h-pt cuts which have been obtained [3] by means of simulations and loaded in the LUT. The choice of these l-pt (p_T ~1 GeV/c) and h-pt (p_T ~2 GeV/c) cuts represents a compromise between background rejection and signal detection efficiency in the mass regions of the J/Ψ and ϒ resonances, respectively.

Results corresponding to the so-called "all-pt" case for which no cut on the deviation is applied at the LUT level are also discussed. Such a case represents the maximum deviation range (minimum p_T) which can be handled by the trigger electronics.

3 SIGNAL AND BACKGROUND

3.1 HEAVY ION COLLISIONS

Parameterizations of the rapidity and transverse momentum distributions for different particle sources are used to evaluate the trigger response. In this section, a brief description of these distributions is given. Moreover, cross-checks have been done using full Monte-Carlo events. PYTHIA events were generated in order to check that kinematical correlations between muons from the same initial heavy quark (charm or bottom) pair do not affect significantly the dimuon trigger rates. HIJING events at various collision centralities were produced for checking in particular that the assumptions made in this note on centrality dependence, based on the Glauber model, are at least reasonable. As a result, no significant difference was found on trigger performance and rates between parameterizations and full Monte-Carlo events.

3.1.1 HADRONIC BACKGROUND

It is known from [2] that muons from pion and kaon decays give the main contribution to the trigger rates. Parameterizations [7] of η (pseudo-rapidity) and p_T distributions obtained with the HIJING event generator are used in this work. It is assumed that these parameterizations do not depend on collision centrality. The charged particle yields per unit of pseudo-rapidity at η=0 are 5800 and 870 for Pb-Pb (b<5 fm) and Ar-Ar (b<3 fm) central collisions, respectively. The generation of hadronic background is limited to the angular range [0-20]° in order to reduce computation time. The corresponding multiplicities are summarized in Table 2.

[1] In this note, "muon" can also be used to denote any track or combination of hits satisfying the muon trigger cuts.

	$N_{\pi^{\pm}}$	$N_{K^{\pm}}$	N_{tot}
Central Pb-Pb collisions (b< 5 fm)	9040	1250	16100
Central Ar-Ar collisions (b< 3 fm)	1840	250	3250

Table 2 : $\pi^{\pm}$, $K^{\pm}$ and total (including neutral particles) mean multiplicities in [0-20]° for central collisions.

Indeed, recent results from RHIC experiments indicate that the actual LHC hadron multiplicities will probably be lower than those listed in Table 2 (see [5] for a summary on this point). This means that this study is based on very conservative assumptions for the hadronic background and hence for the resulting trigger rates (we recall that the systematic error on the muon trigger rate is, at least to some extent, governed by the uncertainty on the yield of the hadronic background).

In addition to decay muons, secondaries from showers produced in the absorbers by pions and kaons may add a significant contribution to the trigger rates. In this work, the hadronic interactions are treated with GEANT-GHEISHA which probably is not the most realistic transport model on the market for hadronic shower development. This is also a source of systematic error which influences the trigger rate. However it was checked that this error stays at an acceptable level because the trigger algorithm is quite robust against this kind of background.

3.1.2 CHARM AND BEAUTY HADRONS

Muons from charm ($D^0, \overline{D}^0, D^{\pm}, D_s^{\pm}, \Lambda_c^{\pm}$) and beauty ($B^0, \overline{B}^0, B^{\pm}, B_s^0, \overline{B}_s^0, \Lambda_b^0, \overline{\Lambda}_b^0$) hadron decay are the main source of high p_T particles reaching the muon trigger detector.

The p_T and y (rapidity) distributions of charm and beauty hadrons, obtained from PYTHIA simulations [8], have been parameterized by means of (3.1). The parameters, given in Table 3, are identical for Pb-Pb and Ar-Ar colliding energies.

$$\frac{d\sigma}{dp_T^2} \propto \left[\frac{1}{1+(p_T/p_0)^2}\right]^n \qquad \frac{d\sigma}{dy} \propto (1-\alpha_0 y^2 - \alpha_1 y^4)^3 \qquad (3.1)$$

	p_0 (GeV/c)	n	α_0	α_1
Charm hadrons	2.25	3.17	$2.43\ 10^{-3}$	$2.31\ 10^{-4}$
Beauty hadrons	6.53	3.59	$1.27\ 10^{-2}$	$2.43\ 10^{-4}$

Table 3 : Parameters for the generation of charm and beauty hadrons.

The mean multiplicity $\overline{N}_{AA}^{hard}$ of hard processes ($Q\overline{Q}$ heavy quark pair production for example) in A-A collisions, in the centrality range $b_1 < b < b_2$ with mean value $< b >$, is calculated in the framework of the Glauber model [9] :

$$\overline{N}_{AA}^{hard}(b_1 < b < b_2) = C_{AA}^{shad}(< b >) \times R_G \times \sigma_{pp}^{hard} \qquad (3.2)$$

$$R_G = \frac{1}{\pi \times (b_2^2 - b_1^2)} \times \int_{b_1}^{b_2} A^2 \times T_{AA}(b)\, d^2b \qquad (3.3)$$

with:

- σ_{pp}^{hard}, the production cross section of the hard process in p-p collisions;
- C_{AA}^{shad}, the nuclear shadowing factor (from [10] with centrality dependence described in [11]);
- R_G, a geometrical factor (3.3) depending on the collision centrality [9];
- T_{AA}, the nuclear overlap function for A-A collisions.

Results for charm and beauty production in central Pb-Pb and Ar-Ar collisions are reported in Table 4 and Table 5, respectively. The values of the parameters of equations (3.2) and (3.3) used to compute the heavy quark multiplicities are also listed in the same tables.

Pb-Pb, $\sqrt{s_{NN}}$ = 5.5 TeV (b<5 fm)	$\sigma_{pp}^{Q\overline{Q}}$ (mb)	R_G (mb^{-1})	C_{PbPb}^{shad}	$\overline{N}_{PbPb}^{Q\overline{Q}}$
$c\overline{c}$ pairs	6.64	23.6	0.65	102
$b\overline{b}$ pairs	0.21	23.6	0.84	4.1

Table 4 : Production cross section in p-p collisions, geometrical and nuclear shadowing factors, and mean number of $c\overline{c}$ and $b\overline{b}$ pairs in central Pb-Pb events.

Ar-Ar, $\sqrt{s_{NN}}$ = 6.3 TeV (b<3 fm)	$\sigma_{pp}^{Q\overline{Q}}$ (mb)	R_G (mb^{-1})	C_{ArAr}^{shad}	$\overline{N}_{ArAr}^{Q\overline{Q}}$
$c\overline{c}$ pairs	7.25	2.31	0.76	12.7
$b\overline{b}$ pairs	0.23	2.31	0.89	0.47

Table 5 : Production cross section in p-p collisions, geometrical and nuclear shadowing factors, and mean number of $c\overline{c}$ and $b\overline{b}$ pairs in central Ar-Ar events.

In average, 204 (25) charm hadrons and 8 (1) beauty hadrons are produced in central Pb-Pb (Ar-Ar) collisions in the full phase-space. The relative percentage between the different hadron species is taken from [8].

3.1.3 QUARKONIA

The p_T distributions for charmonia (J/Ψ, Ψ') and bottomonia (ϒ, ϒ', ϒ'') are extrapolated to LHC energies from CDF measurements, according to a procedure outlined in [11]. The parameterizations are the same as in (3.1), with:

- n =3.83 and p_0 =4.70 GeV/c for charmonia;
- n =3.04 and p_0 =7.75 GeV/c for bottomonia.

The rapidity distributions are taken from the predictions of the Color Evaporation Model [12]. The same kinematical distributions are considered for Pb-Pb and Ar-Ar colliding energies.

Cross sections for charmonia and bottomonia [11] are also calculated in the framework of the Color Evaporation Model. Nuclear shadowing effects are introduced.

For ϕ mesons, the p_T distribution is extrapolated from the pion one according to [13] and the rapidity distribution is the same as the kaon one. The cross section is taken from [1].

Glauber model is also used here for the extrapolation to minimum bias A-A collisions. In this model, the quarkonia cross section $\sigma_{AA}^{[Q\bar{Q}]}$ in minimum bias A-A collisions can be written as:

$$\sigma_{AA}^{[Q\bar{Q}]} = A^2 [\int_0^{b_{max}} T_{AA}(b)\, C_{AA}^{shad}(b) d^2b] \times \sigma_{pp}^{[Q\bar{Q}]} \qquad (3.4)$$

where $\sigma_{pp}^{[Q\bar{Q}]}$ is the quarkonia production cross section in p-p collisions.

3.2 SIGNAL AND BACKGROUND IN P-P

The simulation of p-p collisions is described separately in this short section because it is done in a somewhat different way as compared to the heavy ion case.

3.2.1 MINIMUM BIAS P-P COLLISIONS

Minimum bias p-p events at 14 TeV are produced with PYTHIA 6.214, with kCTEQ5L structure function. This version includes a tuning of the multiplicity distributions according to an extrapolation of CDF data. All kinds of collisions (non-diffractive, single and double diffractive) are considered, except elastic collisions. They correspond to a total cross section of 79 mb.

Particles are propagated in AliRoot using GEANT-FLUKA hadronic cascade code.

3.2.2 QUARKONIA

The same transverse momentum and rapidity distributions as in the heavy ion case are considered.

4 TRIGGER PERFORMANCE

4.1 TRIGGER EFFICIENCY

The trigger efficiency ε_{trig}^{cut} is defined as the ratio of the number of muons satisfying a given trigger p_T cut (all-pt, l-pt or h-pt) to the number of so-called “triggerable” muons. A “triggerable” muon must fire at least 3 out of the 4 possible trigger planes. With such a definition, acceptance (geometrical cuts and absorption of low energy particles) effects cancel out.

4.1.1 SINGLE MUON EFFICIENCY

The single muon trigger efficiency as a function of p_T is shown in Figure 1, for l-pt and h-pt cuts. For l-pt (h-pt) cut, the trigger efficiency is 50% for p_T ~1 GeV/c (2 GeV/c) and reaches a 99% (98%) efficiency plateau for p_T ~3 GeV/c (5 GeV/c).

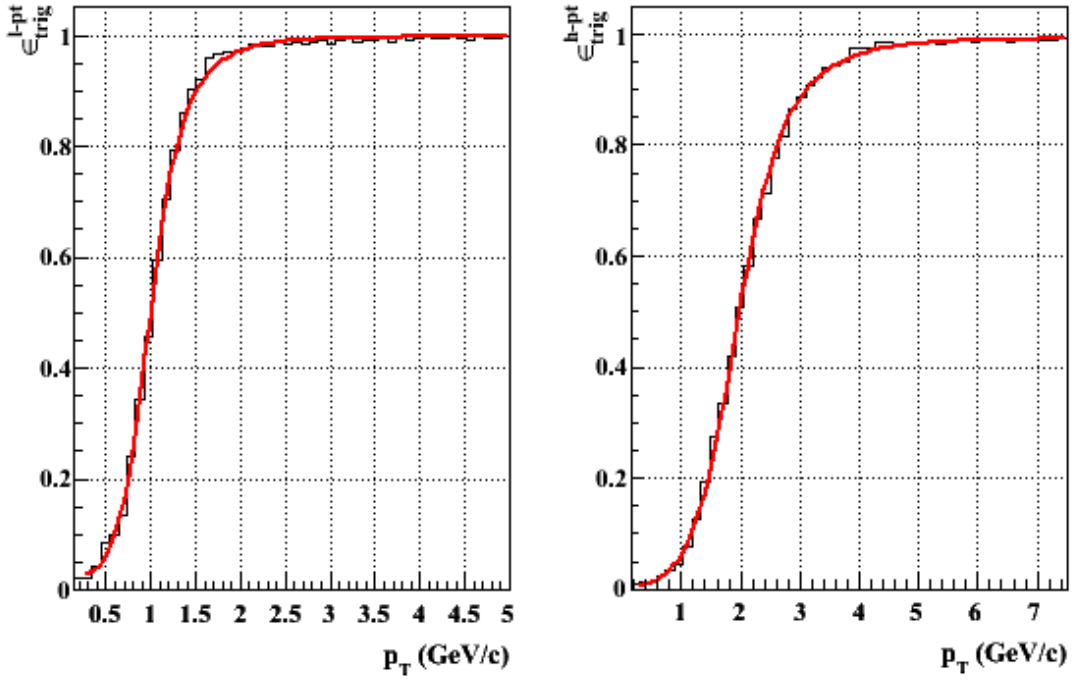

Figure 1: Single muon trigger efficiency as a function of p_T, for l-pt (left) and h-pt (right) cuts. The regular curves are fits, using (4.1).

The single muon trigger efficiency as a function of p_T is fitted using the parameterization:

$$\varepsilon^{cut}_{trig}(p_T) = \alpha \arctan\left[\beta(p_T + \gamma)\right]^6 + \delta \qquad (4.1)$$

The $(\alpha, \beta, \gamma, \delta)$ parameters are given in Table 6, for l-pt and h-pt cuts.

	α	β (GeV/c)$^{-1}$	γ (GeV/c)	δ
$\varepsilon^{l-pt}_{trig}$	0.617	0.717	0.386	0.271 10^{-1}
$\varepsilon^{h-pt}_{trig}$	0.629	0.319	1.215	-0.243 10^{-2}

Table 6 : Parameters of the single muon trigger efficiency fits, for l-pt and h-pt cuts.

Finally, the single muon trigger efficiency in the (p_T,η) plane, for all-pt, l-pt and h-pt cuts is shown in Figure 2. A significant fraction of muons with p_T as low as 0.5 GeV/c is accepted in case of the all-pt cut. Such a cut could be of interest for light colliding systems for which the background is expected to be reduced. The l-pt case, for which the setup was designed and optimized, shows a rather homogeneous response as a function of η. The situation is different for the h-pt cut where the limited resolution of the setup can be observed. Indeed, the structure at η~2.7 (η~3.4) corresponds to the transition between 1 and 2 cm (2 and 4 cm) wide strips of the detector readout planes.

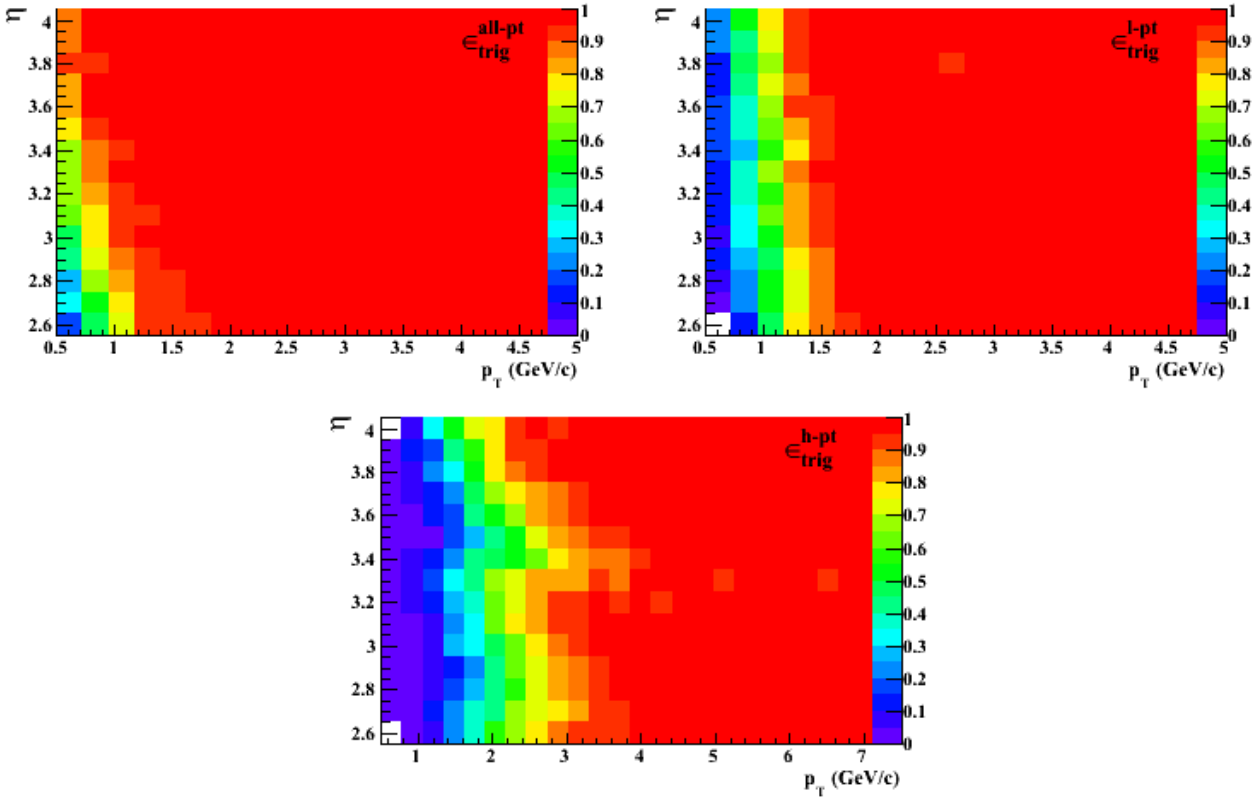

Figure 2 : Single muon trigger efficiency in the (p_T,η) plane, for all-pt (top left), l-pt (top right) and h-pt (bottom) cuts.

4.1.2 EFFICIENCY FOR MUONS FROM PIONS, KAONS, CHARM AND BEAUTY HADRON (HEAVY ION COLLISIONS ONLY)

Pions, kaons, charm and beauty hadrons are produced according to the parameterizations described in section 3 and decay muons are tracked in AliRoot.

The rejection efficiency for each of these muon sources is summarized in Table 7, for different trigger p_T cuts.

	pions, kaons	charm	beauty
$1-\varepsilon^{\text{all-pt}}_{\text{trig}}$	55%	32%	11%
$1-\varepsilon^{\text{l-pt}}_{\text{trig}}$	87%	73%	30%
$1-\varepsilon^{\text{h-pt}}_{\text{trig}}$	96%	92%	64%

Table 7 : Rejection efficiency for “triggerable” muons from pions, kaons, charm and beauty hadron decays, and for all-pt, l-pt and h-pt cuts.

As expected, the rejection efficiency increases as the p_T cut increases. Since muons from beauty are harder than muons from charm which are themselves harder than muons from pion and kaon decays, the rejection efficiency for a given trigger p_T cut evolves accordingly.

4.1.3 EFFICIENCY FOR QUARKONIA

Resonances of the J/Ψ and ϒ families are generated according to the parameterizations described in section 3 and decay muons are tracked in AliRoot. The fraction ε_{trig}^{geo} of "triggerable" dimuons from quarkonia decays is given in Table 8 as well as the fraction ε^{geo} of dimuons in the muon spectrometer geometrical acceptance (the two muons in $2.5<\eta<4$). Therefore, a comparison between ε_{trig}^{geo} and ε^{geo} indicates the magnitude of trigger acceptance effects, for the different quarkonia species. Note that ε^{geo} and ε_{trig}^{geo} depends on the choice of p_T and η parameterizations.

	ϕ	J/Ψ	Ψ'	ϒ	ϒ'	ϒ''
ε_{trig}^{geo}	2.3%	4.8%	4.9%	4.6%	4.3%	4.7%
ε^{geo}	6.0%	5.8%	5.6%	4.9%	4.6%	5.0%

Table 8 : Fraction of "triggerable" dimuons and fraction of dimuons in the muon spectrometer geometrical acceptance, from quarkonia decays.

The quarkonia detection efficiency is reported in Table 9, for different trigger p_T cuts, with the condition that the two decay muons are "triggerable".

	ϕ	J/Ψ	Ψ'	ϒ	ϒ'	ϒ''
$\varepsilon_{trig}^{all-pt}$	57%	90%	93%	97%	98%	98%
$\varepsilon_{trig}^{l-pt}$	13%	71%	81%	97%	98%	98%
$\varepsilon_{trig}^{h-pt}$	2%	22%	28%	88%	90%	91%

Table 9 : Detection efficiency for quarkonia decaying in two "triggerable" muons, for all-pt, l-pt and h-pt cuts. The statistical error is less than 0.5%.

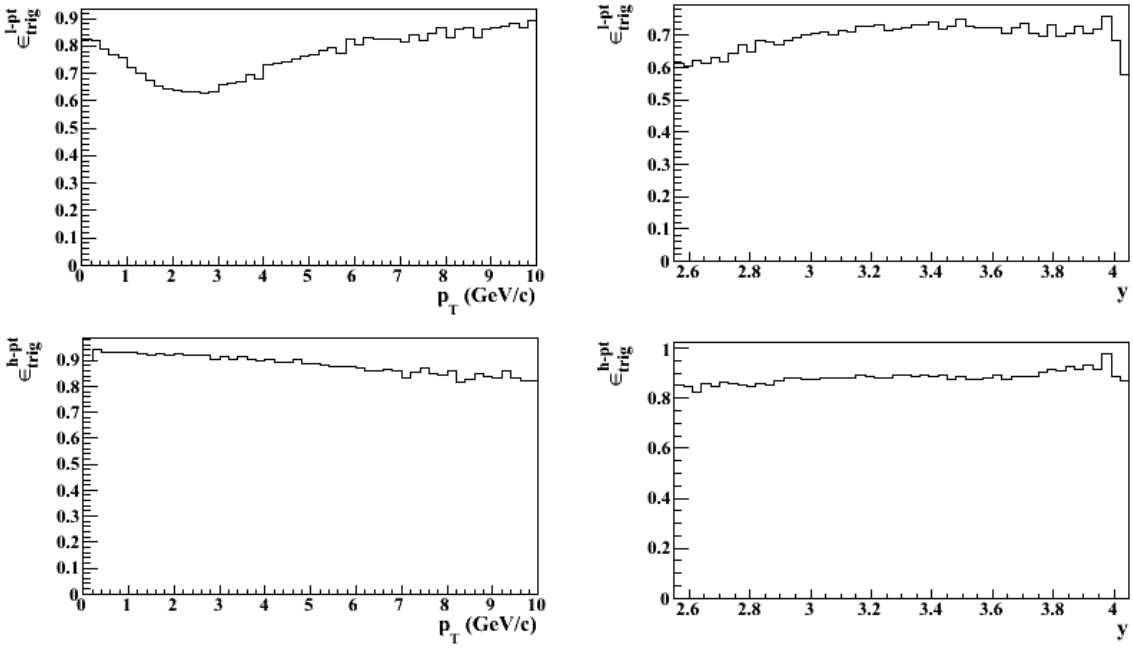

Figure 3 : Trigger efficiency for J/Ψ (top) with l-pt cut and for ϒ (bottom) with h-pt cut as a function of resonance p_T (left) and y (right).

The J/Ψ and ϒ trigger efficiencies are shown in Figure 3 as a function p_T and y of the resonance. The ϒ efficiency is almost flat versus p_T and y. The drop observed at p_T~2.5 GeV/c for the J/Ψ in case of the l-pt cut can be explained by simple kinematical effects.

4.2 QUARKONIA TRIGGER RATES

The quarkonia trigger rates, f_{trig}^{cut}, are calculated from (3.4) for the collision frequencies f^{coll} given in Table 1, after acceptance and trigger efficiency (Table 8 and Table 9) corrections. Results are reported in Table 10, Table 11 and Table 12 for Pb-Pb, Ar-Ar and p-p collisions, respectively. In heavy ion collisions, nuclear effects, other than shadowing, are not included.

		ϕ	J/Ψ	Ψ'	ϒ	ϒ'	ϒ''
	$\sigma_{pp}^{[Q\bar{Q}]}$ (μb)	35000	30.5	4.3	0.50	0.24	0.10
Pb-Pb $\sqrt{s_{NN}}$ = **5.5 TeV**	f_{trig}^{all-pt} ($\times 10^{-3}$ Hz)	1750	1090	19	12.0	3.0	1.9
	f_{trig}^{l-pt} ($\times 10^{-3}$ Hz)	410	850	17	12.0	3.0	1.9
	f_{trig}^{h-pt} ($\times 10^{-3}$ Hz)	56	260	5.7	10.9	2.6	1.7

Table 10 : Triggered quarkonia rates in Pb-Pb collisions for all-pt, l-pt and h-pt cuts.

		ϕ	J/Ψ	Ψ'	ϒ	ϒ'	ϒ''
	$\sigma_{pp}^{[Q\bar{Q}]}$ (μb)	63000	33.1	4.63	0.56	0.28	0.11
Ar-Ar $\sqrt{s_{NN}}$ = **6.3 TeV**	f_{trig}^{all-pt} ($\times 10^{-3}$ Hz)	13700	5090	91	49	12.4	7.4
	f_{trig}^{l-pt} ($\times 10^{-3}$ Hz)	3200	3980	78	49	12.4	7.4
	f_{trig}^{h-pt} ($\times 10^{-3}$ Hz)	420	1210	27	45	11.4	7.0

Table 11 : Triggered quarkonia rates in Ar-Ar collisions for all-pt, l-pt and h-pt cuts.

		ϕ	J/Ψ	Ψ'	ϒ	ϒ'	ϒ''
	$\sigma_{pp}^{[Q\bar{Q}]}$ (μb)	120000	54.1	7.8	1.13	0.52	0.23
p-p $\sqrt{s_{NN}}$ = **14 TeV**	f_{trig}^{all-pt} ($\times 10^{-3}$ Hz)	1350	430	7.9	3.8	0.96	0.57
	f_{trig}^{l-pt} ($\times 10^{-3}$ Hz)	310	340	6.9	3.8	0.96	0.57
	f_{trig}^{h-pt} ($\times 10^{-3}$ Hz)	43	100	2.4	3.5	0.88	0.53

Table 12 : Triggered quarkonia rates in p-p collisions for all-pt, l-pt and h-pt cuts.

4.3 TRIGGER MULTIPLICITY

For each centrality class, pions, kaons, charm and beauty hadrons are generated, event by event, according to their respective multiplicity (Poisson distribution around the mean value). The multiplicity versus centrality, for each source, is supposed to be proportional to the number of

collisions (number of hard processes) calculated in the framework of the Glauber model (3.2) (3.3). Particles are then tracked in AliRoot up to the muon trigger. The mean multiplicity of muons and dimuons above a given p_T cut (m_{μ}^{cut} for single muons, $m_{\mu\mu}^{cut}$ for unlike-sign dimuons) is then known for each source. m_{μ}^{cut} and $m_{\mu\mu}^{cut}$ are of course function of centrality. The total event multiplicity of muons above a given p_T cut is obtained after merging all sources (taking combinatorial effects into account). The values of the multiplicities are summarized in Table 13 for single muons and in Table 14 for unlike-sign dimuons, in central Pb-Pb and Ar-Ar collisions, and in Table 15 for single muons in p-p minimum bias collisions.

		pions, kaons	charm	beauty	Total
Pb-Pb **b < 5 fm**	m_{μ}^{all-pt}	4.84	1.23	0.16	6.25
	m_{μ}^{l-pt}	1.50	0.47	0.11	2.09
	m_{μ}^{h-pt}	0.42	0.13	0.05	0.64
Ar-Ar **b < 3 fm**	m_{μ}^{all-pt}	0.94	0.16	0.02	1.13
	m_{μ}^{l-pt}	0.27	0.06	0.01	0.35
	m_{μ}^{h-pt}	0.07	0.02	0.01	0.10

Table 13 : Mean multiplicity of single muons for all-pt, l-pt and h-pt cuts, in Pb-Pb and Ar-Ar central collisions. Results are given for each source and after merging all sources (last column). The contribution of secondaries from hadronic showers is taken into account for pion and kaon sources and amounts to 30-40% (25-30%) for central Pb-Pb (Ca-Ca) collisions.

	$m_{\mu\mu}^{all-pt}$	$m_{\mu\mu}^{l-pt}$	$m_{\mu\mu}^{h-pt}$
Pb-Pb b < 5 fm	10.34	1.25	0.16
Ar-Ar b < 3 fm	0.34	0.04	0.004

Table 14 : Mean multiplicity of unlike-sign dimuons for all-pt, l-pt and h-pt cuts, in Pb-Pb and Ar-Ar central collisions.

		Total
p-p **Minimum bias**	m_{μ}^{all-pt}	$9.2\ 10^{-3}$
	m_{μ}^{l-pt}	$2.5\ 10^{-3}$
	m_{μ}^{h-pt}	$1.1\ 10^{-3}$

Table 15 : Mean multiplicity of single muons for all-pt, l-pt and h-pt cuts, in p-p minimum bias collisions.

From Table 13, it can be seen that the component from pion and kaon decays gives the main contribution to the trigger multiplicity above any p_T cut.

4.4 TRIGGER RATES

The trigger rate, for a given trigger p_T cut, is given by:

$$f_{trig}^{cut} = f^{coll} \times P_{trig}^{cut} \qquad (4.4)$$

where f^{coll} is the number of collisions per second and P_{trig}^{cut} is the trigger probability (dimuon or single muon). Both f^{coll} and P_{trig}^{cut} depend on the collision centrality.

The mean collision rate $\bar{f}_{AA}^{coll}$ in the centrality range $(b_1 < b < b_2)$, for A-A collisions, is given by:

$$\bar{f}_{AA}^{coll} = < L > \times \pi \, (b_2^2 - b_1^2) \qquad (4.5)$$

where $< L >$ is the mean luminosity, with values given in Table 1.

The trigger decision (hence the trigger probability P_{trig}^{cut}) is obtained directly from the AliRoot simulation, event by event after the merging process (see section 4.3). The trigger probability versus impact parameter is reported in Figure 4 in Pb-Pb collisions, for single muons and unlike-sign dimuons.

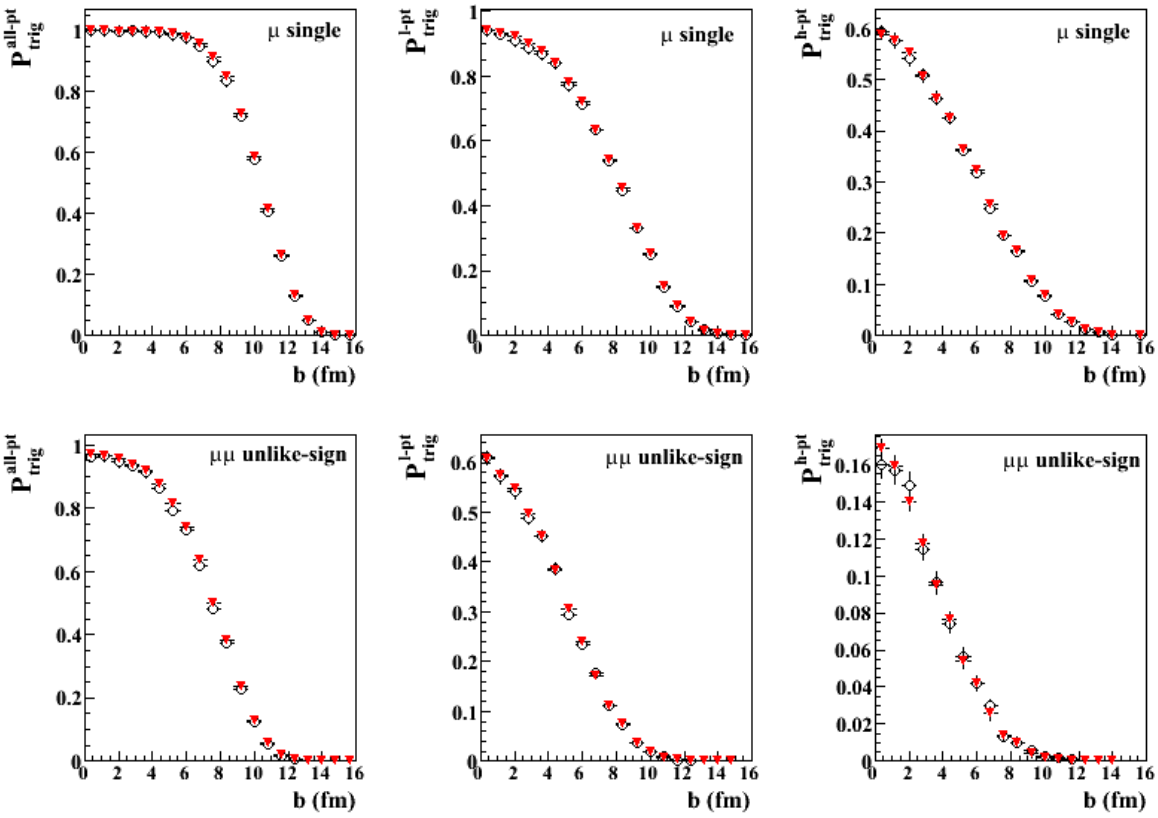

Figure 4: Trigger probability versus impact parameter for Pb-Pb collisions, for single muons (top) and dimuons (bottom), and for all-pt, l-pt and h-pt cuts (from left to right). The trigger probability (open circles), from the event by event simulation, is compared to Poissonian distributions (triangles).

The trigger probability P_{trig}^{cut}, from the event by event simulation, is compared to Poissonian distributions for single muons (4.6) and unlike-sign dimuons (4.7).

$$P_{\mu-Poiss}^{cut} = 1 - \exp(-m_{\mu}^{cut}) \qquad (4.6)$$

$$P_{\mu\mu-Poiss}^{cut} = \left[1 - \exp(-\frac{m_{\mu}^{cut}}{2})\right]^2 \qquad (4.7)$$

As expected, the agreement is very good. Such a Poissonian behaviour could help for calculating rapidly the trigger probability and rate, without repeating the full simulation process, providing only that muon multiplicity m_{μ}^{cut} versus impact parameter is known. For example, this could be useful for an estimation of the trigger rates in case of other hadronic background conditions.

Finally, the trigger rates for collisions with impact parameter b smaller than b_{max} are displayed in Figure 5 as a function of b_{max} for Pb-Pb collisions and in Figure 6 for Ar-Ar collisions. A summary of the trigger rates, in minimum bias collisions, is given in Table 16. The rates in p-p do not include any contribution from beam-gas induced background because a large fraction of such events should be rejected by means of the V0 detector.

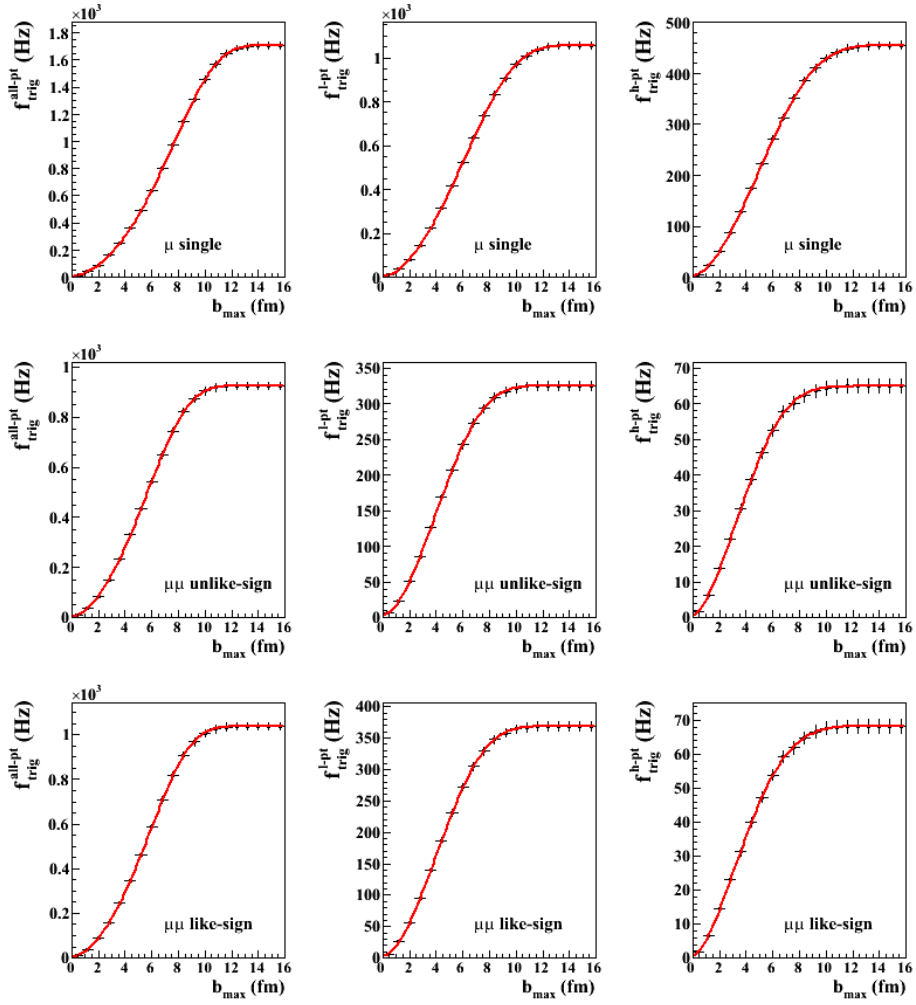

Figure 5 : Impact parameter integrated trigger rates, in Pb-Pb collisions, for single muons (top), unlike-sign dimuons (middle) and like-sign dimuons (bottom), and for all-pt, l-pt and h-pt cuts (from left to right). The curves are fits of the simulation points.

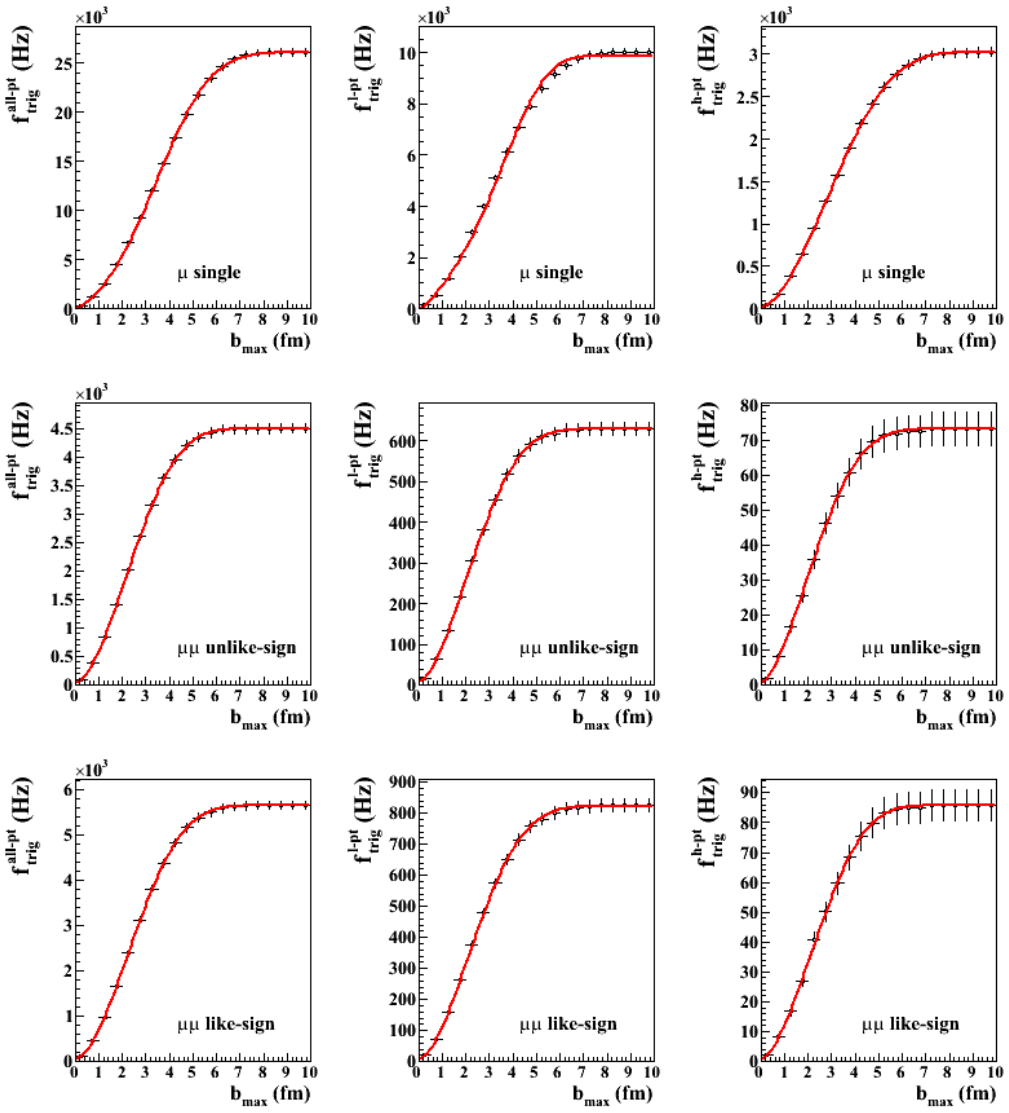

Figure 6 : Impact parameter integrated trigger rates, in Ar-Ar collisions, for single muons (top), unlike-sign dimuons (middle) and like-sign dimuons (bottom), and for all-pt, l-pt and h-pt cuts (from left to right).
The curves are fits of the simulation points.

	f^{coll} (Hz)	f^{all-pt}_{trig} (Hz)	f^{l-pt}_{trig} (Hz)	f^{h-pt}_{trig} (Hz)
Pb-Pb , single muons	$4\ 10^3$	1700	1100	450
Pb-Pb , unlike-sign dimuons		930	330	65
Ar-Ar , single muons	$1.5\ 10^5$	26000	10000	3000
Ar-Ar , unlike-sign dimuons		4500	630	73
p-p , single muons	$2\ 10^5$	1850	510	225
p-p , unlike-sign dimuons		27 (±10)	10 (±5)	5 (±3)

Table 16: Trigger rates for Pb-Pb, Ar-Ar and p-p minimum bias collisions,
for single muons and unlike-sign dimuons, and for all-pt, l-pt and h-pt cuts.

The muon trigger rates must be limited to about 1 kHz in order to keep the dead-time of muon event readout to a low value. Such a rate of 1 kHz should fit the bandwidth of the ALICE muon HLT. The outcomes of these simulations show that dimuon rates fulfil such a requirement, already for the l-pt cut. It should be also possible to register a large sample of single muons for the h-pt cut.

5 CONCLUSION

The muon trigger performance has been updated. The final results are remarkably in good agreement with those of 1999 [1], considering all the evolutions which have occurred in between.

The trigger efficiency on quarkonia (Table 9) is high for resonances of the J/Ψ and ϒ families. The dimuon trigger rates (Table 16) are within requirements.

As shown in Table 13, the trigger rates in central Pb-Pb collisions are dominated by hadronic background. Any sizeable modification of the magnitude of this source, which is basically unknown within a factor two, would of course affect the values of the trigger rates. Nonetheless, preliminary data taking scenarii for ALICE muon physics can be elaborated on the basis of the results presented in this note.

REFERENCES

[1] ALICE collaboration, Technical Design Report of the dimuon forward spectrometer, CERN/LHCC 99-22 (1999).

[2] Olivier Roig, PhD thesis, University Blaise Pascal of Clermont-Fd (1999), PCCF T 9910.

[3] Benoit Forestier, PhD thesis, University Blaise Pascal of Clermont-Fd (2003), PCCF T 0305.

[4] Frédéric Yermia, PhD thesis, University Blaise Pascal of Clermont-Fd and University of Torino (2005).

[5] ALICE collaboration, ALICE Physics Performance Report (Volume 1), CERN/LHCC 2003-049 (2003).

[6] G. Blanchard, P. Crochet and P. Dupieux, the local trigger electronics of the ALICE dimuon trigger, ALICE-EN 2003-010 (2003).

[7] A. Morsch and K. Eggert, Onium production in heavy-ion collisions at the LHC - Signals and backgrounds in the two-muon channel, ALICE-INT/PHY 95-05 (1995).

[8] N. Carrer and A. Dainese, Charm and beauty production at LHC, ALICE-INT 2003-019 v.3, hep-ph/0311225.

[9] R.J. Glauber and G. Matthiae, Nucl. Phys. B21 135 (1970).

[10] K.J. Eskola, V.J. Kolhinen and C.A. Salgado, Eur. Phys. J. C9 61 (1999).

[11] ALICE collaboration, ALICE Physics Performance Report (Volume 2), CERN/LHCC 2005-030 (2005).

[12] M. Bedjidian et al., Hard probes in heavy ion collisions at the LHC: heavy flavour physics, hep-ph/0311048.

[13] M. Bourquin and M. Gaillard, Nucl. Phys. 114B (1976) 334.